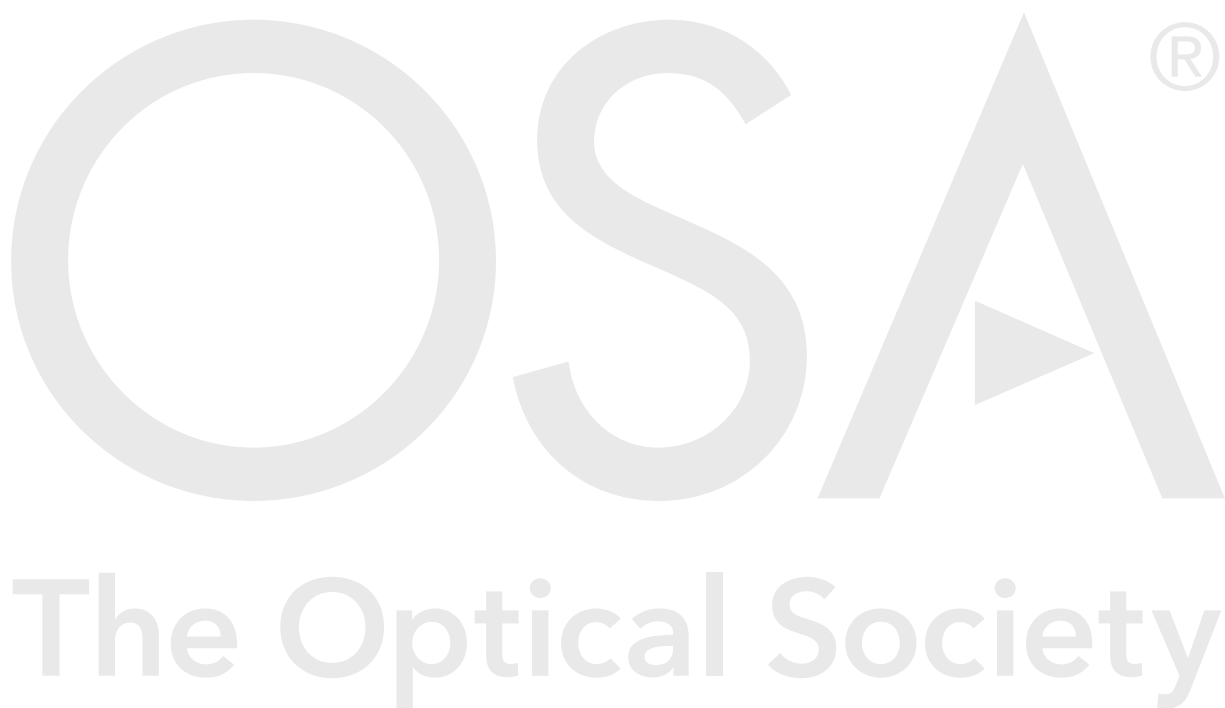


To be published in Optics Letters:

Title: A 40 Gb/s indoor optical wireless system enabled by a cyclically arranged optical beamsteering
Authors: Xuebing Zhang, Yu Liu, Zizheng Cao, Fan Li, Zhaohui Li, Rand Ismaeel, Gilberto Brambilla, Y
Accepted: 11 January 18
Posted 11 January 18
Doc. ID: 314317

Published by



A 40 Gb/s indoor optical wireless system enabled by a cyclically arranged optical beamsteering receiver

XUEBING ZHANG,¹ YU LIU,² ZIZHENG CAO,^{1,*} FAN LI,³ ZHAOHUI LI,³ R. ISMAEEL,⁴ G. BRAMBILLA,⁴ Y. CHEN,⁴ A.M.J. KOONEN¹

¹Eindhoven University of Technology, NL 5600 MB Eindhoven, Netherlands

²State Key Laboratory on Integrated Optoelectronics, Institute of Semiconductors, Chinese Academy of Sciences, Beijing, 100083, China

³State Key Laboratory of Optoelectronic Materials and Technologies and School of Electronics and Information Technology, Sun Yat-sen University, Guangzhou 510275, China

⁴Optoelectronics Research Centre, University of Southampton, Southampton SO17 1BJ, U.K.

*Corresponding author: z.cao@tue.nl

Received XX Month XXXX; revised XX Month, XXXX; accepted XX Month XXXX; posted XX Month XXXX (Doc. ID XXXXX); published XX Month XXXX

Indoor optical wireless communication with optical beamsteering capability is currently attracting a lot of attention. One major two dimensional (2D) optical beamsteering scheme is realized by 2D grating or its active counterpart which is usually based on spatial light modulator (SLM). However, there is a fundamental trade-off between the field-of-view (FoV) and power efficiency due to the inherent feature of gratings. In this paper, we propose a new class of 2D beamsteering, named cyclically arranged optical beamsteering (CAO-BS) which can break such trade-off. Traditional 2D gratings extend the optical beam in Cartesian coordinate (1D grating in horizontal + 1D grating in vertical), while CAO-BS extend optical beam in polar coordinate (1D grating + angular rotation). Since only 1D grating is engaged, the power efficiency increases with the number of grating lobes reduced. In polar coordinate, the angle rotation tuning in a SLM is quasi-continuous in a full 2π range. The CAO-BS is demonstrated at the receiving end in an indoor experimental system. The FoV is 18° by 360° in polar coordinate without any additional mechanical part. Based on the CAO-BS, 40 Gbit/s On-Off Keying (OOK) data is also successfully transmitted over 1km single mode fibre and 0.5 m free space. © 2017 Optical Society of America

OCIS codes: (060.2605) Free-space optical communication; (070.1170)

Analog optical signal processing; (070.6110) Spatial filtering;

(070.6120) Spatial light modulators.

<http://dx.doi.org/10.1364/OL.99.099999>

Recently, indoor optical wireless communication (OWC) technology is widely recognised as a popular access method due to its prominent bandwidth advantage [1]. Nowadays, fibre-to-the-home unlocks unlimited bandwidth in the fibre end, however, the

amount of bandwidth accessible to the end user is still limited by the radio frequency in the air. For example, mm-wave radio-over-fibre (RoF) techniques can largely reduce the complexity but the available bandwidth is still limited to a few GHz at the mm-wave band. [3-4]. With the available fibre links of FTTH, OWC at 1550 nm band is complementary to radio for high-speed short-range communication in the Fifth Generation (5G) networks [2]. Next to the 5G radio communication, OWC can boost the aggregate capacity to Tb/s level [5]. In order to track the mobile terminal users indoor, precise alignment between the transmitter and receiver is of demand. Therefore, beam reconfigurable receiver with a large total field-of-view (FoV) is interesting. Moreover, the allowed infrared power is limited due to the safety regulation, such receiver should be power efficient. To this end, beamsteering is of demand.

Spatial light modulator (SLM) is applied for beamsteering in indoor OWC systems [6-10]. The SLM could steer optical beam without mechanical movement. Comparing other means, the SLM has highly repeatable performance, high tolerance towards environment variance (e.g. vibration). The SLM also does not limit the signal's bandwidth [7] and is robust to laser wavelength drifts. F. Feng et al. have demonstrated a maximum 3° beam shifting in free space link by using an SLM [7]. Later, A. Gomez et al. extend the FoV to 60° by introducing an extra lens system as an angle magnifier (AM) [8]. Such AM concept is attractive since it can directly increase the FoV of all kinds of systems. However, so far, these SLM-based methods merely demonstrate two-dimensional (2D) beamsteering by using the 2D grating in Cartesian coordinate. For one-dimensional (1D) gratings, if we assume its number of grating lobes is N , when extending it to 2D, the number of grating lobes is $N \times N$. As the number increase, its power efficiency decreases. The covered range of grating lobes, or in other word, the Field-of-View (FoV) is traded off with the power efficiency. Additionally, it is difficult to implement beamsteering at (quasi-)

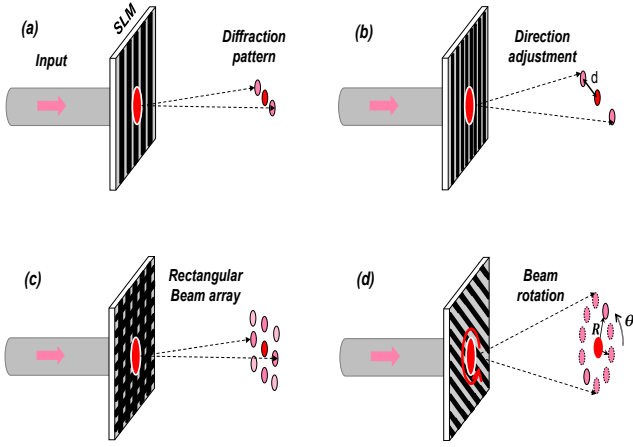


Fig. 1. The concept of SLM-based cyclically arranged optical beamsteering; (a) the general 1D grating diffraction; (b) grating pitch adjustment; (c) 2D beamsteering using 2D grating; (d) cyclically arranged optical 2D beamsteering. SLM: spatial light modulator; d: The distance between central and first order spots;

continuous angle because the order of gratings is discrete. This results in only certain discrete angles in the steering area which can be accessed. Here, we propose another 2D beamsteering scheme named cyclically arranged optical beamsteering (CAO-BS) to break the trade-off between FoV and power efficiency. Traditional 2D gratings extend the optical beam in Cartesian coordinate (1D grating in horizontal + 1D grating in vertical), while CAO-BS extend the optical beam in Polar coordinate (1D grating + angular rotation). Since only 1D grating is engaged, the power efficiency increases with the number of grating lobes reduced. In polar coordinate, the angle rotation tuning in a SLM is quasi-continuous within a full 2π range. Even though the idea of CAO-BS has never been explored for indoor OWC systems, a similar idea to use rotation as a degree of freedom for beamsteering is studied in Risley Prisms [11-12]. Based on the CAO-BS concept, a FoV of 18° is experimentally demonstrated by using a reflective SLM, where the FoV can be enlarged to almost 140° when an AM proposed in [8] is applied. The OWC transmission of 40Gbit/s On-Off Keying (OOK) data is also experimentally demonstrated over 1km standard single mode fibre and 0.5 m free space. This quasi-continuous $\pm 9^\circ$ FoV greatly releases the pressure from alignment and thus provides a promising solution for indoor OWC systems.

Fig. 1 shows the concept of SLM-based 2D CAO-BS. The general diffraction pattern is presented in Fig. 1a. By changing the grating pitch, we could alter the pointing direction of the first order beam, which is the common meaning of 1D beamsteering as shown in Fig. 1b. In the 1D case, the operation principles of CAO-BS and the conventional method are the same. As shown in Fig. 1c, for a traditional 2D beamsteering, a 1D grating is extended to a 2D grating, while for CAO-BS, a cyclical rotation is applied to the 1D grating as shown in Fig. 1d. This avoids further power splitting in another dimension, which enables higher power efficiency.

Even though the 1D grating can be quasi-continuously rotated in the angle dimension, the angle 1D grating is still discrete due to the limitation of pixel size of SLM just like the conventional method, leaving some disabled pointing directions. This is the main drawback of these SLM-based methods. As suggested in [7], for an

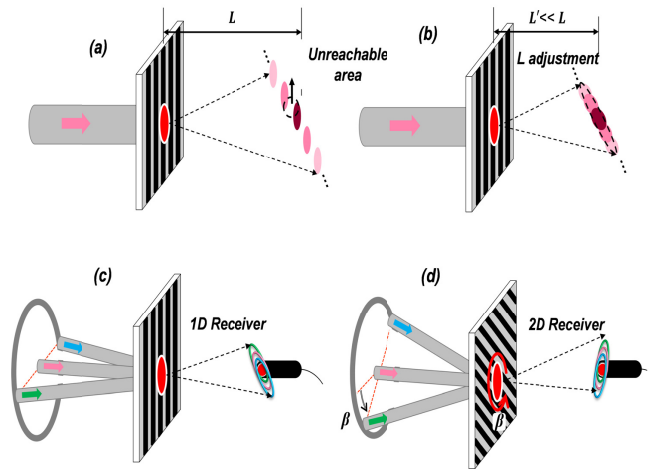


Fig. 2. The principle of the SLM-based receiver that supports 2D continuous-angle beamsteering (a) general grating diffraction; (b) demonstration of continuous beam; (c) 1D receiver; and (d) 2D receiver. L: The distance between diffraction beam and grating; β : The angle between the incident plane and the horizontal plane.

SLM, the maximum deflection angle α of the first order in full angle is determined by pixel pitch Δ of SLM device and laser wavelength λ , which is presented as $\alpha = \lambda/\Delta$. In the reported work, the Δ of the SLM is $\sim 20 \mu\text{m}$ and the wavelength is 1060 nm and thus the maximum α is ~ 3.04 degree. In practice, Δ is the smallest adjustable size. In order to fill in the area between two discrete angles, we propose a new structure that can meet this requirement as shown in Fig. 2.

Fig. 2a illustrates the general diffraction pattern used in the proposed receiving approach. Compared to the conventional SLM-based beamsteering [7], CAO-BS utilizes higher order spots instead of eliminating them, thus extending the angle range. L is the distance between SLM and receiver, which is an essential factor in our scheme. As we discussed above, we could clearly see an unreachable area between central spot and first order grating lobes. However, when we reduce L to L' ($L' \ll L$), for instance around 10 mm in our experiment, the grating lobes can be quite close to the central spot as shown in Fig. 2b. If we decrease L further, the uniformness will be better. When all grating lobes at the orders of interest are then close enough to fall in the coupling region (aperture) of collimator, a wide-FoV receiver without blind spots is realized as shown in Fig. 2c. Optical beams at different directions (illustrated by different colours) are projected to the grating. The grating elliptical rings with different colours represent input signals at different angles. When the angle of the input signal changes along one direction (eg. horizontal direction in Fig. 2c), the linear beam will shift a certain angle in the same direction as well but there is always a part of the beam that falls in the aperture of the collimator. This radiated beam ensures a stable optical connection without blind area for a wide receiving angle. Fig. 2d shows the 2D principles. For arbitrary input light within the FoV of 1D grating, the grating is rotated to match the input direction by updating the phase profile of the SLM. For instance, when an incident plane rotates β degree anticlockwise, the grating angle should have the same rotation to make sure it is perpendicular to the new incident plane as shown in Fig. 2d. In this experiment, we demonstrate the optical receiver based on a reflective SLM

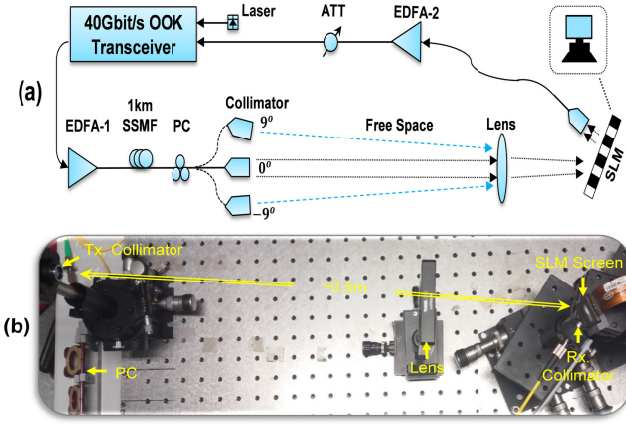


Fig. 3. Experimental setup (a) the whole transmission system and (b) the real free space link. ATT: optical attenuator; EDFA: erbium-doped fibre amplifier; SSMF: standard single mode fibre; PC: polarization controller.

produced by HOLOEYE (PLUTO Phase Only SLM). It should be pointed that for our receiver structure, the reflective SLM is same as transmissive type in terms of function [13].

The experimental setup is illustrated in Fig. 3 (a). A laser with narrow bandwidth (<100 kHz) is employed for the optical carrier with the wavelength of 1550 nm. 40Gbit/s OOK signal is generated from a commercial transmitter (SHF10000B) and then amplified by an Erbium-doped fibre amplifier (EDFA-1) before transmitting onto a 1-km standard SMF. Here, the 1-km standard SMF corresponds the distance from a central controlling room to the users' room in an indoor scenario. The SLM used here is a polarization-sensitive device, hence, a polarization controller (PC) is introduced to optimize the modulation efficiency of the SLM. Then the light is fed into a transmitting collimator (NA=0.28) and transmitted over 0.5 m free space link. This free space link is used to emulate the distance between access point and terminal users. A lens with the focal length of 200 mm is employed to adjust the spot size. A more compact receiver can be constructed with a specially designed lens (system). The reflective SLM has 1920×1080 active pixels and $8 \mu\text{m}$ pixel pitch. The spatially modulated lightwave is then collected by a smaller collimator (NA=0.16) and coupled into the SMF. The distance between this collimator and the SLM is ~ 10 mm. To compensate the insertion loss including the misalignments-caused loss, a pre-amplifier (EDFA-2) is used. An optical attenuator is introduced to measure the bit error rate (BER) versus received optical power curves.

The experimental results are analysed as shown in Fig. 4, 5, and 6. As discussed in Fig. 2 (d), the uniformness of reflective beams are first evaluated by a movable multimode fibre with a small aperture ($\varnothing=62.5 \mu\text{m}$). Such small aperture allows the accurate measurement of power distribution with high spatial resolution. The location and angle of the receiving 'collimator' (multimode fibre) is adjusted while fixing the transmitting collimator. The fibre is moved in steps of 0.5 mm within a full range of ~ 10 mm. A slight angular adjustment is implemented to optimize the power collection. The results are shown in Fig. 4. The input power is set at 9 dBm, and the measured output power is between -34.5 dBm and -37.8 dBm. The variation is less than 3.3 dB, which suggests a quite

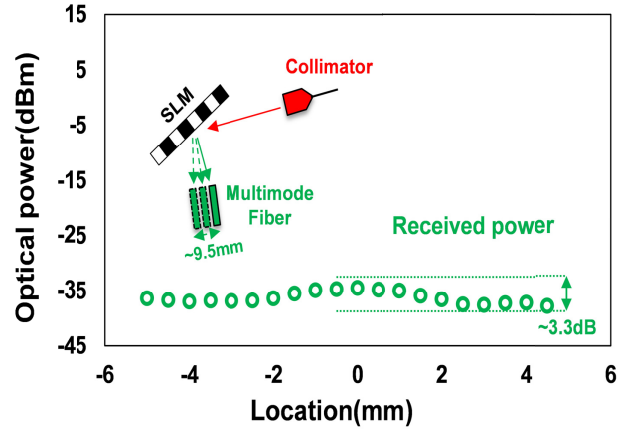


Fig. 4. Power distribution of the linear beam.

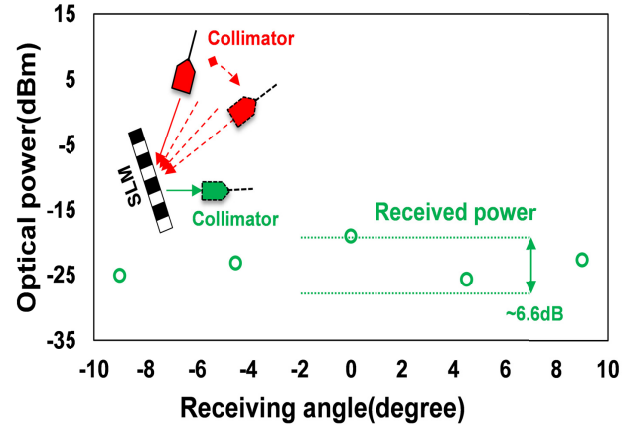


Fig. 5. Received power versus receiving angle curves.

uniform power distribution along a line. As expected, there is no apparent blind spot.

Then we replace the multimode fibre with the receiving collimator with NA of 0.16. The other conditions are maintained, including the input power and the configurations of the free-space optical system. The transmitting collimator is then tuned at five different angles of -9° , -4.5° , 0° , 4.5° and 9° . The measured powers are -25.01 dBm, -23.1 dBm, -19 dBm, -25.6 dBm and -22.7 dBm respectively, as shown in Fig. 5. It should be pointed out that these powers are measured before EDFA-2. The power variation is less than 6.6dB, which shows our proposed method could provide relatively stable operations within the FoV of 18° . The power loss is ~ 33 dB in our experiment mainly due to misalignments. Firstly, in the receiving architecture, the very short distance (~ 10 mm or even smaller) between SLM and receiving collimator requires a small-sized collimator or the collimator will block the incident light from the transmitter. Coupling light into the smaller collimator is more difficult due to the small aperture. Secondly, the fixed ~ 10 mm distance and the linear beam with large divergence angle are more likely to cause the mismatch of divergence angle, which will lead to a large power loss. Actually, if the active aperture of the collimator is increased or a photodetector is substituted for the collimator, the power loss could be reduced a lot, but there are still

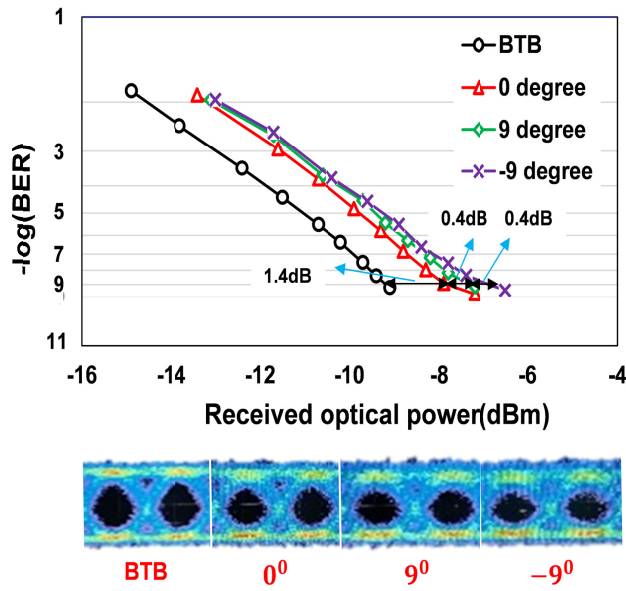


Fig. 6. Received power versus receiving angle curves and measured eye diagrams.

some problems to overcome. Also, the free optic system is not fully optimized. In the future, a well-designed optic system can decrease the power loss.

The bit error rate (BER) performance of the system is tested by using 40Gbit/s OOK signal. In this experiment, we select -9° , 0° and 9° incident angles to evaluate the system's transmission performance. The BER curves are shown in Fig. 6. At the BER threshold of 1×10^{-9} , the power penalty at the angle of -9° , 0° and 9° are -7.8, -7.4, and -7.0 dBm, respectively. As a reference, the power is -9.2 dBm for the case of optical back-to-back (BTB) condition. The sensitivity at 0° angle is the highest among all the three transmission cases, showing a 1.4 dB degradation compared with the reference. This is mainly because of the introduction of the boosting amplifier (EDFA-1) and pre-amplifier (EDFA-2). The difference of receiver sensitivity between at the angles of 0° and 9° are 0.4 dB. The performance at the angle of -9° is with 0.8 dB decrease compared to that at the angle of 0° . This coincides well with the imbalanced received power shown in Fig. 5. Such imbalance may be caused by the angle-dependent efficiency of the SLM. As shown in the lower part of Fig. 6, the eye diagrams for optical BTB, and at the angles of -9° , 0° and 9° are all measured at the power of 0 dBm. No drastic changes in rising/falling edges is observed, which suggests that the optical manipulation does not affect the received electrical bandwidth.

To conclude this paper, we proposed a novel 2D beamsteering scheme named CAO-BS to break the trade-off between FoV and power efficiency. Different from traditional 2D gratings, CAO-BS extend optical 1D beamsteering to 2D beamsteering in Polar coordinate (1D grating + angular rotation). Since only 1D grating is engaged, the power efficiency increases with the number of grating lobes reduced. Moreover, in polar coordinate, the angle rotation tuning in a SLM is quasi-continuous in a full 2π range. Based on this concept, we propose a novel beamsteering receiver with quasi-continuous angle utilizing a SLM and a conventional collimator. A FoV of 18° by 360° in polar coordinates is

experimentally demonstrated in the CAO-BS receiver without using mechanical movement. This FoV could be further extended to $\sim 140^\circ$ by 360° in polar coordinates when an angle magnifier as proposed is applied. In addition, 40 Gbit/s bit-rate OOK transmission experiment is demonstrated over 1km standard single mode fibre and 0.5 m free space link. We believe that this technique provides a promising solution for indoor OWC systems.

Funding. ERC FP-7 advanced grant BROWSE (agreement: 291632), the National Natural Science Foundation of China (Nos. 61575186 and 61635001), and open fund from State Key Laboratory of Advanced Optical Communication Systems Networks, China.

References

1. D. C. O'Brien, M. Katz, P. Wang, K. Kalliojarvi, S. Arnon, M. Matsumoto, R. J. Green and S. Jivkova, in *Wireless world research forum* 2005., pp. 1-22
2. M. Ayyash, H. Elgala, A. Khreishah, V. Jungnickel, T. Little, S. Shao, M. Rahaim, D. Schulz, J. Hilt, R. Freund, IEEE Communications Magazine, vol. 54(2), pp.64-71 (2016).
3. A.M.J. Koonen and E. Tangdiongga, Journal of Lightwave Technology, vol. 32(4), pp.591-604 (2014).
4. Z. Cao, J. Yu, H. Zhou, W. Wang, M. Xia, J. Wang, Q. Tang and L. Chen, Journal of Optical Communications and Networking, vol. 2(2), pp.117-121 (2010).
5. H. Huang, G. Xie, Y. Yan, N. Ahmed, Y. Ren, Y. Yue, D. Rogawski, M. J. Willner, B. I. Erkmen, K. M. Birnbaum and S. J. Dolinar, Opt. Lett., vol. 39(2), pp. 197-200 (2014).
6. C. J. Henderson, D. G. Leyva and T. D. Wilkinson, Free space adaptive optical interconnect at 1.25 Gb/s, with beam steering using a ferroelectric liquid-crystal SLM. Journal of Lightwave Technology, 24(5), p.1989 (2006).
7. F. Feng, I. H. White and T. D. Wilkinson, Journal of Lightwave Technology, vol. 31(12), pp.2001-2007 (2013).
8. A. Gomez, K. Shi, C. Quintana, M. Sato, G. Faulkner, B. C. Thomsen and D. O'Brien, IEEE Photon. Technol. Lett., 27(4), pp.367-370 (2015).
9. A. Gomez, C. Quintana, M. Sato, G. Faulkner and D. O'Brien, International Society for Optics and Photonics 2016 (SPIE OPTO 2016) (pp. 97720Q-97720Q).
10. A. Gomez, C. Quintana, M. Sato, G. Faulkner and D. O'Brien, International Society for Optics and Photonics 2016 (SPIE OPTO 2016), pp. 97720Q-97720Q.
11. Oh. C. Kim, J. Muth, S. J. Serati and M. J. Escuti, IEEE Photonics Technology Letters, 22(4), pp.200-202 (2010).
12. A. Li, W. Sun, W. Yi and Q. Zuo, Optics express, 24(12), pp.12840-12850 (2016).
13. J. Harriman, S. Serati and J. Stockley, In Proc. SPIE, vol. 5930, pp. 605-614 (2005).

Full reference

1. D. C. O'Brien, M. Katz, P. Wang, K. Kalliojarvi, S. Arnon, M. Matsumoto, R. J. Green and S. Jivkova, "Short-range optical wireless communications." In *Wireless world research forum*, pp. 1-22 (2005).
2. M. Ayyash, H. Elgala, A. Khreishah, V. Jungnickel, T. Little, S. Shao, M. Rahaim, D. Schulz, J. Hilt, R. Freund, "Coexistence of WiFi and LiFi toward 5G: Concepts, opportunities, and challenges." *IEEE Communications Magazine*, vol. 54(2), pp.64-71 (2016).
3. A.M.J. Koonen and E. Tangdionga, "Photonic home area networks." *Journal of Lightwave Technology*, vol. 32(4), pp.591-604 (2014).
4. Z. Cao, J. Yu, H. Zhou, W. Wang, M. Xia, J. Wang, Q. Tang and L. Chen, "WDM-RoF-PON architecture for flexible wireless and wire-line layout." *Journal of Optical Communications and Networking*, vol. 2(2), pp.117-121 (2010).
5. H. Huang, G. Xie, Y. Yan, N. Ahmed, Y. Ren, Y. Yue, D. Rogawski, M. J. Willner, B. I. Erkmen, K. M. Birnbaum and S. J. Dolinar, "100 Tbit/s free-space data link enabled by three dimensional multiplexing of orbital angular momentum, polarization, and wavelength," *Opt. Lett.*, vol. 39(2), pp. 197–200 (2014).
6. C. J. Henderson, D. G. Leyva and T. D. Wilkinson, "Free space adaptive optical interconnect at 1.25 Gb/s, with beam steering using a ferroelectric liquid-crystal SLM." *Journal of Lightwave Technology*, 24(5), p.1989 (2006).
7. F. Feng, I. H. White and T. D. Wilkinson, "Free space communications with beam steering a two-electrode tapered laser diode using liquid-crystal SLM." *Journal of Lightwave Technology*, vol. 31(12), pp.2001-2007 (2013).
8. A. Gomez et al., "Beyond 100-Gb/s indoor wide field-of-view optical wireless communications." *IEEE Photon. Technol. Lett.*, vol. 27(4), pp.367-370 (2015).
9. A. Gomez, K. Shi, C. Quintana, M. Sato, G. Faulkner, B. C. Thomsen and D. O'Brien, "Beyond 100-Gb/s indoor wide field-of-view optical wireless communications." *IEEE Photon. Technol. Lett.*, 27(4), pp.367-370 (2015).
10. A. Gomez, C. Quintana, M. Sato, G. Faulkner and D. O'Brien, "Point-to-multipoint holographic beamsteering techniques for indoor optical wireless communications." *International Society for Optics and Photonics 2016 (SPIE OPTO 2016)*, pp. 97720Q-97720Q.
11. Oh. C. Kim, J. Muth, S. J. Serati and M. J. Escuti, "High-throughput continuous beam steering using rotating polarization gratings." *IEEE Photonics Technology Letters*, 22(4), pp.200-202 (2010).
12. A. Li, W. Sun, W. Yi and Q. Zuo, "Investigation of beam steering performances in rotation Risley-prism scanner." *Optics express*, 24(12), pp.12840-12850 (2016).
13. J. Harriman, S. Serati and J. Stockley, "Comparison of transmissive and reflective spatial light modulators for optical manipulation applications." In *Proc. SPIE*, vol. 5930, pp. 605-614 (2005).